Symmetry-enriched Bose-Einstein condensates in a spin-orbit-coupled bilayer system

Jia-Ming Cheng,[1] Xiang-Fa Zhou,[1,2] Zheng-Wei Zhou,[1,2,*] Guang-Can Guo,[1,2] and Ming Gong[1,2,†]
[1]CAS Key Laboratory of Quantum Information, University of Science and Technology of China, Hefei 230026, People's Republic of China
[2]Synergetic Innovation Center of Quantum Information and Quantum Physics, University of Science and Technology of China, Hefei 230026, People's Republic of China

(Received 4 July 2017; published 22 January 2018)

We consider the fate of Bose-Einstein condensation with time-reversal symmetry and inversion symmetry in a spin-orbit-coupled bilayer system. When these two symmetry operators commute, all the single-particle bands are exactly twofold degenerate in the momentum space. The scattering in the twofold-degenerate rings can relax the spin-momentum locking effect from spin-orbit-coupling interaction and thus can realize the spin-polarized plane-wave phase even when the interparticle interaction dominates. When these two operators anticommute, the lowest two bands may have the same minimal energy, but with totally different spin structures. As a result, the competition between different condensates in these two energetically degenerate rings can give rise to different stripe phases with atoms condensed at two or four collinear momenta. We find that the crossover between these two cases is accompanied by the excited band condensation when the interference energy can overcome the increased single-particle energy in the excited band. This effect is not based on strong interaction and thus can be realized even with moderate interaction strength.

DOI: 10.1103/PhysRevA.97.013625

I. INTRODUCTION

The synthetic gauge potentials in ultracold atoms have attracted much attention in recent years [1–7]. In the Abelian gauge potential the neutral atoms can experience a light-induced commutative vector potential [8–10], thus many interesting phases in charged electrons from the Lorentz force can be simulated using neutral atoms [11–19], including the integer and fractional quantum Hall effects [20–22]. The non-Abelian potential, such as the spin-orbit-coupling (SOC) effect, is more intriguing due to the spin-momentum locking effect. It not only fundamentally changes the fate of Bose-Einstein condensation (BEC) in Bose gases [23–30], but may also give rise to topological phases in Fermi gases [31–35]. Thus the synthetic gauge potentials in ultracold atoms have opened a totally new avenue in exploring fundamental physics [36–44]; to date, at least nine experimental groups have realized the SOC in different atoms [45–55].

The SOC can modify the topology of a single-particle band from a minimal point at $\mathbf{k} = 0$ to a degenerate ring at $|\mathbf{k}| \neq 0$ in two spatial dimensions. In the latter case it is impossible to develop the BEC without interaction due to the infinite degeneracy of the ground-state space. However, interaction can force all atoms to occupy only a few momenta and the ground state is then determined by the minimized interaction energy, which favors either the spin-balanced plane-wave (PW) phase when $c_{12} < 1$ or the spin fully polarized PW phase without SOC and the standing-wave (SW) phase with SOC when $c_{12} > 1$ (c_{12} denotes the ratio between interparticle and intraparticle scattering strengths) [24]. This principle has been applied to understand the exotic BEC in various circumstances [23–30] in which it is impossible to form the PW phase when the interparticle interaction dominates.

We go beyond the above no-go regime by considering the BEC in two degenerate rings in a spin-orbit-coupled bilayer system. (i) When all the bands are twofold degenerate due to the commutation relation between the time-reversal operator and the inversion operator, the scattering in the degenerate space can relax the spin-momentum locking effect and the spin-polarized PW phase can be realized even when $c_{12} > 1$. The spin polarization is controlled by the interlayer tunneling. (ii) When the two operators anticommute, the condensates in the two lowest energetically degenerate rings with distinct spin structures can give rise to different spin-balanced collinear stripe (ST) phases occupying two or four momenta. (iii) The crossover between the above two cases is accompanied by the condensation in the excited band due to the interference effect, which can be realized even with moderate interaction strength.

II. MODEL AND HAMILTONIAN

We consider a bilayer system with Rashba SOC [55]. Along the perpendicular direction, the tunneling between the two layers is assumed to be spin dependent $t_\uparrow = -t_\downarrow = t$, which can be realized by fast modulation of the optical lattice [56–58]. The single-particle Hamiltonian reads $H_0 = \int d\mathbf{r}\, \psi^\dagger(\mathbf{r})\mathcal{H}_0\psi(\mathbf{r})$, with $\mathcal{H}_0 = \frac{\mathbf{k}^2}{2m} + \frac{\lambda}{m}\sigma_0 \otimes \mathbf{k}\cdot\boldsymbol{\sigma} - \sigma_x \otimes \tilde{t}$ and $\tilde{t} = \mathrm{diag}\{t_\uparrow, t_\downarrow\}$, under the basis $\psi(\mathbf{r}) = [\psi_{1\uparrow}(\mathbf{r}), \psi_{1\downarrow}(\mathbf{r}), \psi_{2\uparrow}(\mathbf{r}), \psi_{2\downarrow}(\mathbf{r})]^T$. Here λ is the SOC strength, $\mathbf{k} = (k_x, k_y)$, and $\boldsymbol{\sigma} = (\sigma_x, \sigma_y)$ are Pauli matrices. The experimental realization of this model based on the spin-dependent optical lattice was discussed in Ref. [59]. Notice that the spin-dependent tunneling introduces a relative π phase between the two spin components, which is equivalent to introducing a minus sign to the SOC coefficients between

*zwzhou@ustc.edu.cn
†gongm@ustc.edu.cn

the two layers. Thus the above model can be mapped to the following model by a unitary rotation:

$$\mathcal{H}_0 = \frac{\mathbf{k}^2}{2m} + \frac{\lambda}{m}\sigma_z \otimes \mathbf{k}\cdot\sigma - t\sigma_x \otimes \sigma_0 \tag{1}$$

for $\psi(\mathbf{r}) = [\psi_{1\uparrow}(\mathbf{r}), \psi_{1\downarrow}(\mathbf{r}), \psi_{2\uparrow}(\mathbf{r}), -\psi_{2\downarrow}(\mathbf{r})]^T$. We neglect the interlayer interaction, thus the interacting Hamiltonian can be written as [29,30]

$$\mathcal{V}_{\rm int} = \frac{g}{2}\sum_{i=1,2}\int d\mathbf{r}\big[n_i^2(\mathbf{r}) + 2(c_{12}-1)n_{i\uparrow}(\mathbf{r})n_{i\downarrow}(\mathbf{r})\big], \tag{2}$$

where $n_{i\sigma}(\mathbf{r}) = \psi_{i\sigma}^\dagger(\mathbf{r})\psi_{i\sigma}(\mathbf{r})$ and $n_i(\mathbf{r}) = \sum_\sigma n_{i\sigma}(\mathbf{r})$. In the following, Eq. (1) is used in our simulation and the total Hamiltonian $\mathcal{H} = \mathcal{H}_0 + \mathcal{V}_{\rm int}$.

This model is intriguing due to the presence of time-reversal symmetry $\mathcal{T}$ and inversion symmetry $\mathcal{I}$ between the two layers defined as [60]

$$\mathcal{T} = \sigma_0 \otimes i\sigma_y K, \quad \mathcal{I} = \sigma_x \otimes \sigma_0, \tag{3}$$

where K is the complex conjugate operator. The combination of the above two operators enables the definition of a new antiunitary operator $T = \mathcal{I}\cdot\mathcal{T} = \sigma_x \otimes i\sigma_y K$, which satisfies

$$T\mathcal{H}_0(\mathbf{k})T^{-1} = \mathcal{H}_0(\mathbf{k}), \quad T^2 = -1. \tag{4}$$

The above result is based on the fact that $\mathcal{I}$ and $\mathcal{T}$ commute, i.e., $[\mathcal{I},\mathcal{T}] = 0$. The Kramers theorem ensures that all the bands at each $\mathbf{k}$ are exactly twofold degenerate. In the single-layer system [24], these two symmetry operators anticommute, thus does not have the above feature. For the model in Eq. (1) we have

$$\epsilon^\pm(\mathbf{k}) = t_0\left\{\left(\frac{k}{\lambda}\right)^2 \pm \left[4\left(\frac{k}{\lambda}\right)^2 + t'^2\right]^{1/2}\right\}, \tag{5}$$

with $t' = t/t_0$ and $t_0 = \lambda^2/2m$. Hereafter t_0 is used as the basic energy scale throughout this work. The topology of the ground-state space is controlled by t' and the degenerate rings with radius $k = \lambda\sqrt{1 - t'^2/4}$ will shrink to a point at $\mathbf{k} = 0$ when $t' \geqslant 2$. When $t' > 2$, the two degenerate eigenvectors at $\mathbf{k} = 0$ read

$$\phi_1^\eta(\mathbf{r}) = (1,\eta,1,\eta)^T/2, \quad \eta = \pm, \tag{6}$$

with the single-particle energy $\epsilon_{\rm min}^- = -t't_0$. When $t' < 2$, the wave functions at the degenerate rings are

$$\phi_{2\mathbf{k}}^\eta(\mathbf{r}) = (\gamma_\eta e^{-i\theta_{\mathbf{k}}}, \eta\gamma_\eta, \gamma_{-\eta}e^{-i\theta_{\mathbf{k}}}, \eta\gamma_{-\eta})^T e^{i\mathbf{k}\cdot\mathbf{r}}/2, \tag{7}$$

with $\gamma_\eta = [1 - \eta(1 - t'^2/4)^{1/2}]^{1/2}$, $e^{i\theta_{\mathbf{k}}} = (k_x + ik_y)/k$, and $\epsilon_{\rm min}^- = -t_0(1 + t'^2/4)$.

III. PHASE DIAGRAM

We combine the variational analysis and imaginary-time-evolution method (confined in a weak trap) to determine the fate of BEC by minimizing the total energy per particle $\mathcal{E}_g = \mathcal{E}_0 + \mathcal{E}_{\rm int}$, where $\mathcal{E}_0 = \int d\mathbf{r}\,\phi^*(\mathbf{r})\mathcal{H}_0\phi(\mathbf{r}) = \epsilon_{\rm min}^-$ defines the single-particle energy [61]. The interaction is essential to develop BEC over a degenerate space via the order-by-disorder mechanism, which singles out a ground state from the degenerate space. These two methods yield the same phase diagram in Fig. 1 as a function of c_{12} and t'.

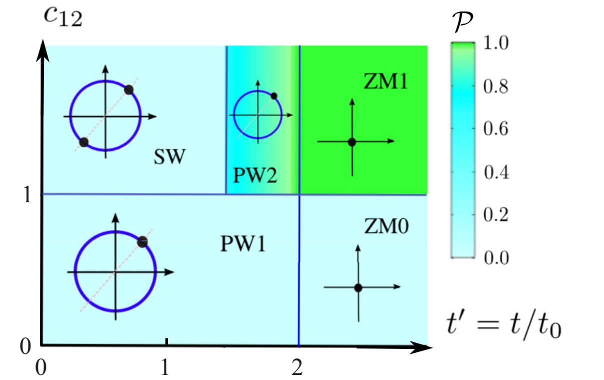

FIG. 1. Phase diagram for BEC in two identical degenerate rings. In each phase the condensate is denoted by a solid cycle (or cycles) and $\mathcal{P} = |\langle\sigma_z\rangle|$ defines the corresponding spin polarization.

First we consider the case when all the atoms are condensed at $\mathbf{k} = 0$, in which the wave function should be a superposition of the two orthogonal states in Eq. (6). We find (a) when $c_{12} < 1$, the ground state is a spin-balanced phase (denoted by ZM0) in Fig. 1,

$$\psi_{\rm ZM0}(\mathbf{r}) = |\alpha|\phi_1^+(\mathbf{r}) \pm i|\beta|\phi_1^-(\mathbf{r}), \tag{8}$$

with $\mathcal{E}_{\rm ZM0} = -t + g(1 + c_{12})/8$ for arbitrary α and β. All components have the same weight and $\mathcal{P} = |\langle\psi_{\rm ZM0}|\sigma_z|\psi_{\rm ZM0}\rangle| = 0$. In contrast, in case (b) when $c_{12} > 1$, the ground state is fully spin polarized (denoted by ZM1 in Fig. 1),

$$\psi_{\rm ZM1}(\mathbf{r}) = [\phi_1^+(\mathbf{r}) \pm \phi_1^-(\mathbf{r})]/\sqrt{2}, \tag{9}$$

in which $\mathcal{P} = |\langle\sigma_z\rangle| = 1$ and $\mathcal{E}_{\rm ZM1} = -t + g/4$. The transition between ZM0 and ZM1, $\mathcal{E}_{\rm ZM1} = \mathcal{E}_{\rm ZM0}$, yields the boundary at $c_{12} = 1$, across which it is a first-order transition due to the discontinuity of $\mathcal{E}$ with respect to c_{12}.

Next we turn to the twofold-degenerate rings with $t' < 2$. When $t' \to 0$, we can recover the results in previous literature where a first-order transition from the PW phase (denoted by PW1) to the SW phase (denoted by SW) is expected at $c_{12} = 1$ [see Fig. 2(a)]. Without extra degeneracy the spin-momentum locking effect prohibits tuning of spin polarization for a given $\mathbf{k}$, thus when $c_{12} > 1$, the SW phase should be favored to reduce the interparticle energy. This locking effect can be relaxed in the degenerate rings due to the possible scattering between the two states in Eq. (7) in the degenerate space, where the spin polarization in the PW phase can still be tuned in a wide range by the superposition principle. For instance, when $t' \to 2^-$, a spin-polarized state ($\mathcal{P} = |\langle\sigma_z\rangle| \to 1$) can be realized by a basis rotation. Thus the PW phase (denoted by PW2) is still allowed when $c_{12} > 1$.

The PW2 phase beyond the no-go regime can be understood by minimizing the total energy using the two wave functions in Eq. (7). We find that when $c_{12} < 1$, the wave function takes the form

$$\psi_{\rm PW1}(\mathbf{r}) = [\phi_{2\mathbf{k}}^+(\mathbf{r}) \pm i\phi_{2\mathbf{k}}^-(\mathbf{r})]/\sqrt{2}, \tag{10}$$

with energy $\mathcal{E}_{\rm PW1} = g(1 + c_{12})/8 - t_0(1 + t'^2)/4$, and $\mathcal{P} = 0$, thus this phase is spin balanced. However, when $c_{12} > 1$, the wave function reads

$$\psi_{\rm PW2}(\mathbf{r}) = [\phi_{2\mathbf{k}}^+(\mathbf{r}) \pm \phi_{2\mathbf{k}}^-(\mathbf{r})]/\sqrt{2}, \tag{11}$$

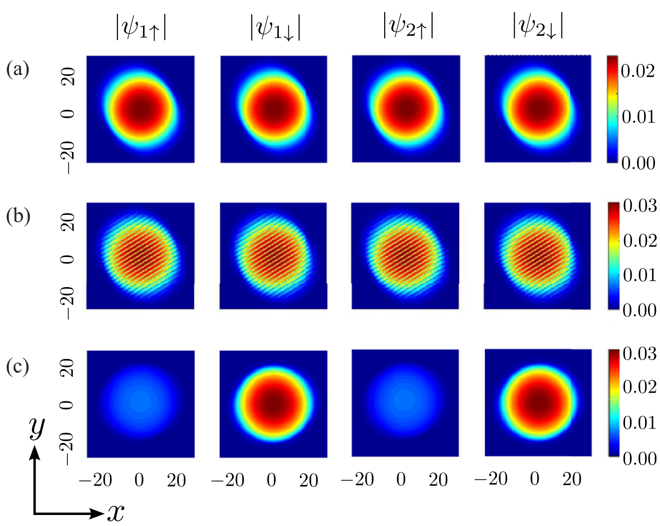

FIG. 2. Ground-state densities in a trap for (a) the PW1 phase with $(t',c_{12}) = (1.0,0.8)$, (b) the SW phase with $(1.0,1.2)$, and (c) the PW2 phase with $(1.8,1.2)$. In the imaginary-time-evolution simulation, $\lambda = 2$, $g = 100$, $\delta = -1$, and $m = 1$.

with $\mathcal{E}_{\rm PW2} = g[(1 + c_{12}) + (1 - c_{12})t'^2/4]/8 - t_0(1 + t'^2/4)$, and spin polarization $\mathcal{P} = t'/2$ [see the wave functions in Fig. 2(c)].

In the SW phase, the wave function should be a superposition of all the possible waves [Eq. (7)] with momenta $\mathbf{k}_1$ and $\mathbf{k}_2$. By direct numerical minimization we find

$$\psi_{\rm SW}(\mathbf{r}) = [\psi_{\rm PW1}(\mathbf{r}) + e^{i\vartheta}\mathcal{T}\psi_{\rm PW1}(\mathbf{r})]/\sqrt{2}, \tag{12}$$

with $\mathcal{E}_{\rm SW} = g'[(1 + c_{12}) + (1 - c_{12})/2]/8 - t_0(1 + t'^2/4)$ [see Fig. 2(b)]. The phase boundary between the SW and PW2 phases is determined by $\mathcal{E}_{\rm SW} = \mathcal{E}_{\rm PW2}$, which yields $t' = \sqrt{2}$. Thus we have the full phase diagram in Fig. 1.

IV. BEC IN TWO ENERGETICALLY DEGENERATE RINGS

We now generalize this idea to another intriguing condition when the two layers have slightly different SOC strengths, say, $\lambda_1 = \lambda$ and $\lambda_2/\lambda_1 = \delta$. We still work in the rotated picture in Eq. (1), thus $\delta = -1$ corresponds to identical rings discussed in Fig. 1. In this case the two identical rings will be divided into two rings. We consider

$$\mathcal{H}_0' = \begin{pmatrix} \frac{(\mathbf{k}+\lambda_1\boldsymbol{\sigma})^2}{2m} - \frac{\lambda_1^2}{2m} & -t \\ -t & \frac{(\mathbf{k}+\lambda_2\boldsymbol{\sigma})^2}{2m} - \frac{\lambda_2^2}{2m} \end{pmatrix}. \tag{13}$$

This model admits a different inversion symmetry $\mathcal{I}' = \sigma_0 \otimes \sigma_z$. With the method in Eq. (4), we can define another antiunitary operator $T' = \mathcal{I}' \cdot \mathcal{T} = \sigma_0 \otimes \sigma_x K$, with

$$T'\mathcal{H}_0'(\mathbf{k})T'^{-1} = \mathcal{H}_0'(\mathbf{k}), \quad T'^2 = +1. \tag{14}$$

Here $\mathcal{I}'$ anticommutes with $\mathcal{T}$, i.e., $\{\mathcal{I}',\mathcal{T}\} = 0$, similar to that in the single-layer system. This symmetry means that for any eigenvector $\mathcal{H}_0'\phi = E\phi$, $T'\phi$ should also be its eigenvector with the same eigenenergy. The uniqueness of the solution requires $T'\phi = \phi$ upon a global phase difference, which ensures that all the wave functions should be fully spin balanced, i.e.,

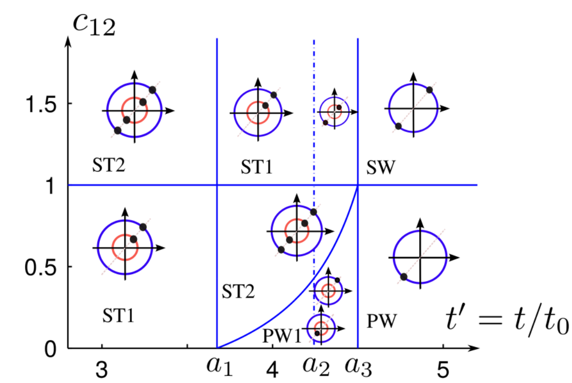

FIG. 3. Phase diagram for BEC in two energetically degenerate rings when $\lambda_2 = -2\lambda_1$. Here $a_1 = (1-\delta)^2/\sqrt{6}$, $a_2 = \sqrt{-\delta(1-\delta)^2}$, and $a_3 = (1-\delta)^2/2$. In all phases, the spin polarization $\mathcal{P} = 0$.

$\mathcal{P} = |\langle\phi|\sigma_z|\phi\rangle| = 0$. By a proper unitary rotation we find

$$\mathcal{H}_0' \to \begin{pmatrix} \epsilon(k_+ + \delta\lambda\sigma_z) & 0 \\ 0 & \epsilon(k_- + \delta\lambda\sigma_z) \end{pmatrix} - t\sigma_0 \otimes \sigma_x, \tag{15}$$

where $\epsilon(k) = k^2/2m$, $k_\pm = k + (\lambda_1 + \lambda_2)/2$, and $\delta\lambda = (\lambda_1 - \lambda_2)/2$. The upper block and the lower block are identical upon a momentum shift $k \to k - (\lambda_1 + \lambda_2)$, thus they should be degenerate in their eigenvalues upon the same momentum shift and

$$\epsilon^i(\mathbf{k}) = t_0\left[q_i^2 + (1-\delta)^2/4 - \sqrt{(1-\delta)^2 q_i^2 + t'^2}\right], \tag{16}$$

with $i = 1,2$ and $q_i = k/\lambda + (-1)^i(1+\delta)/2$. The time-reversal symmetry ensures that $\epsilon^i(k) = \epsilon^i(-k)$ and the momentum translation ensures $\epsilon^1(k) = \epsilon^2[k - (\lambda_1 + \lambda_2)]$, thus the two rings should have the same minimal energy. This new degeneracy leads to strong competition between different possible condensates. The corresponding phase diagram in this degenerate space is presented in Fig. 3.

The topology of the single-particle bands is controlled by the parameter $\chi = (1-\delta)^2 - 2t'$, which has two energetically degenerate rings when $\chi > 0$; otherwise it is a single ring. In case (a), when $\chi > 0$, the two rings have radii $k_\pm = \{\pm(1+\delta)/2 + (1-\delta)[1 - 4t'^2/(1-\delta)^4]^{1/2}/2\}\lambda$, with the same single-particle energy $\epsilon_{\rm min}(\mathbf{k}) = \epsilon^1_{\rm min}(\mathbf{k}_1) = \epsilon^2_{\rm min}(\mathbf{k}_2) = t_0[-t'^2/(1-\delta)^2]$. The corresponding wave functions for these two rings are

$$\varphi_{\mathbf{k}_1} = [x_+(e^{i\theta_{\mathbf{k}_1}},-1), x_-(e^{i\theta_{\mathbf{k}_1}},-1)]^T e^{i\mathbf{k}_1\cdot\mathbf{r}}, \tag{17}$$

$$\varphi_{\mathbf{k}_2} = [x_-(e^{i\theta_{\mathbf{k}_2}},1), x_+(e^{i\theta_{\mathbf{k}_2}},1)]^T e^{i\mathbf{k}_2\cdot\mathbf{r}}, \tag{18}$$

where $x_\mp = \{1 \mp [1 - 4t'^2/(1-\delta)^4]^{1/2}\}^{1/2}/2$. Obviously, $T'\varphi_{\mathbf{k}_i} = \varphi_{\mathbf{k}_i}$ and $\mathcal{P} = 0$. The fate of BEC depends strongly on the scattering between and in the rings, which may occupy one, two, or four collinear momenta in one ring or two rings. We find three interesting cases. (i) For the PW phase (PW1)

$$\psi_{\rm PW1} = \varphi_{\mathbf{k}_1} \quad \text{or} \quad \psi_{\rm PW1} = \varphi_{\mathbf{k}_2} \tag{19}$$

and the corresponding total energy is $\mathcal{E}_{\rm PW1} = -t_0t'^2/(1-\delta)^2 + g(1+c_{12})\{1/4 - t'^2/[2(1-\delta)^4]\}$. (ii) For the stripe (ST1) phase with two collinear momenta ($\mathbf{k}_1 \parallel \mathbf{k}_2$), the wave function can be written as

$$\psi_{\mathrm{ST1}} = [\varphi_{\mathbf{k}_1} + \exp(i\vartheta)\varphi_{\mathbf{k}_2}]/\sqrt{2}, \tag{20}$$

where $\mathcal{E}_{\mathrm{ST1}} = -t_0 t'^2/(1-\delta)^2 + g\{(1+c_{12})/8 + (1-c_{12})t'^2/[4(1-\delta)^4]\}$. (iii) When both rings are occupied by four momenta $\{\mathbf{k}_1,\mathbf{k}_2,-\mathbf{k}_1,-\mathbf{k}_2\}$ for the ST2 phase, the wave function can be written as

$$\psi_{\mathrm{ST2}} = (\psi_{\mathrm{ST1}} + e^{i\vartheta'}\mathcal{T}\psi_{\mathrm{ST1}})/\sqrt{2}, \tag{21}$$

where $\mathcal{E}_{\mathrm{ST2}} = \mathcal{E}_{\mathrm{ST1}} + g(1-c_{12})\{1/4 - 3t'^2/[2(1-\delta)^4]\}/4$. The SW phase in Fig. 1 is absent here when $\chi > 0$ due to its slightly higher energy than these three cases. These minimized energies are used to determine the phase diagram presented in Fig. 3 for $\chi < 0$ (for $t' < a_3$). The boundary between PW1 and ST2 is determined by $2(3+5c_{12})t'^2 = (1+3c_{12})(1-\delta)^4$ and the boundary between ST1 and ST2 is determined by $t' = a_1$ and $c_{12} = 1$. Notice that for $t' \in (a_2,a_3)$, the ground state may have two different condensates with the same energy.

In case (b) when $\chi \leqslant 0$ the ground state is only made by a single ring. The minimal energy is determined by $\epsilon^2_{\min}(\mathbf{k}) = t_0[(1-\delta)^2/4 - t']$ at $k = -(1+\delta)\lambda/2$ and its wave function is

$$\varphi_{\mathbf{k}} = (e^{i\theta_{\mathbf{k}}},1,e^{i\theta_{\mathbf{k}}},1)^T e^{i\mathbf{k}\cdot\mathbf{r}}/2. \tag{22}$$

For the PW phase, the total energy is $\mathcal{E}_{\mathrm{PW}} = t_0[(1-\delta)^2/4 - t'] + g(1+c_{12})/2$ and for the SW phase,

$$\psi_{\mathrm{SW}} = (\varphi_{\mathbf{k}} + e^{i\theta}\mathcal{T}\varphi_{\mathbf{k}})/\sqrt{2}, \tag{23}$$

with $\mathcal{E}_{\mathrm{SW}} = \mathcal{E}_{\mathrm{PW}} + g(1-c_{12})/4$. We find that the PW phase is favored when $c_{12} < 1$; otherwise the SW phase is favored, similar to that reported in previous literature [23–30].

These phases in two separate rings can be understood from the result in degenerate rings in Fig. 1 by adiabatically switching δ off from $\delta = -1$, in which each condensate in momentum $\mathbf{k}$ may split into two condensates with different momenta $\mathbf{k}_\pm$. This explains excellently most of the phases in Figs. 1–3 except the ST2 phase and the PW1 phase. In the PW1 phase, only one momentum $\mathbf{k}$ is allowed due to the reason discussed in Fig. 1; in contrast, in the ST2 phase the competition between different possible condensates is more complicated. This regime has a special physical consequence, discussed below.

V. EXCITED BAND CONDENSATION FROM THE INTERFERENCE EFFECT

Notice that $\lim_{\delta\to -1} a_{2,3} \to 2$, thus these two boundaries can be adiabatically tuned to the phase boundary at $t' = 2$ in Fig. 1. However, $\lim_{\delta\to -1} a_1 \to 4/\sqrt{6} \neq \sqrt{2}$, thus the boundary controlled by a_1 cannot be tuned to the phase boundary of the SW and PW2 phases in Fig. 1. This is attributed to the condensate in the excited band from the interference effect, which can be realized even for moderate interaction strength. To this end, let us assume that

$$\psi = \alpha\varphi'_{1\mathbf{q}_1} + \beta\varphi'_{2\mathbf{q}_2}, \tag{24}$$

where it is no longer necessary to restrict $\mathbf{q}_1$ and $\mathbf{q}_2$ to the degenerate rings. We have

$$\mathcal{E}(\mathbf{q}_1,\mathbf{q}_2) = T + V + (1-c_{12})\mathcal{A}[(\alpha^*\beta)^2 + \mathrm{H.c.}]\delta_{\mathbf{q}_1,\mathbf{q}_2}, \tag{25}$$

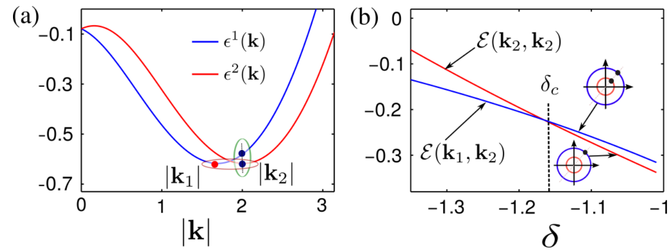

FIG. 4. (a) Two lowest single-particle bands for $\delta = -1.16$. The atoms can occupy either two rings or the ground state and first excited band in a single ring. (b) Ground-state energies for these two different condensates. The parameters are $\lambda = 2$, $t' = 1.2$, $g = 2$, $c_{12} = 0.5$, and $\delta_c = -1.16$.

where $T = |\alpha|^2\epsilon^1(\mathbf{q}_1) + |\beta|^2\epsilon^2(\mathbf{q}_2)$ represents the kinetic energy, $\mathcal{A}$ is a constant depending on the details of the wave function, and V is the interacting energy discussed before. The last term, arising from the interference effect, is most relevant to our discussion here. When $\mathbf{q}_1 = \mathbf{q}_2$, the interference between the particles can further lower the total energy when $\alpha^*\beta \simeq i/2$ for $c_{12} < 1$ and $\alpha^*\beta \simeq 1/2$ for $c_{12} > 1$. This lowered energy may overcome the increased single-particle energy $|\beta|^2[\epsilon^2(\mathbf{q}_2) - \epsilon^1(\mathbf{q}_1)]$ when condensed partially in the excited band [see Fig. 4(a)]. The outer ring always has energy lower than the inner ring, thus letting

$$\mathcal{E}(\mathbf{k}_1,\mathbf{k}_2) = \mathcal{E}(\mathbf{k}_2,\mathbf{k}_2), \tag{26}$$

we are able to determine the critical boundary between condensates in degenerate rings and the excited band as

$$\delta_c = -1 + [-B - (B^2 - 2AB)^{1/2}]/2A, \tag{27}$$

with $A = [5(c_{12}-1)gt'^2 - 8(t'^2-4)\lambda^2]/128$ and $B = (c_{12}-1)gt'^2/32$. For the data in Fig. 4(b), the predicted boundary is $\delta_c = -1.1615$, which is in excellent agreement with the numerical result. When $\delta = -1$, the excited band condensate automatically evolves to the phase diagram in Fig. 1. This condensate effect is totally different from the condensate in excited states from the strong repulsive interaction [62,63]. The regime for excited band condensation can be further enhanced by increasing the scattering strength and thus, in principle, can be observed in a wide range. We also notice that $\mathcal{P} = 0$ when $c_{12} < 1$ and $\mathcal{P} \neq 0$ when $c_{12} > 1$ from the results in Fig. 1, which provides an important basis for experimental detection of the excited band condensation.

VI. DISCUSSION AND CONCLUSION

Symmetries play an essential role in condensed matter physics, especially for the topological phases [64,65]. The artificial bilayer systems have been widely explored in recent years for the realization of different exotic phases [66–68]. In this work, we demonstrated that the time-reversal symmetry and inversion symmetry can introduce some extra degeneracy to the single-particle bands in a spin-orbit-coupled bilayer system, which can fundamentally change the fate of BEC in the degenerate space. These results provide a route for the realization of exotic BEC using the state-of-art techniques in ultracold atoms. Notice that these condensates are not protected by symmetries in the sense of topology, thus they will not be immediately destroyed upon weak symmetry breaking.

ACKNOWLEDGMENTS

M.G. was supported by the National Youth Thousand Talents Program (Grant No. KJ2030000001), the USTC start-up funding (Grant No. KY2030000053), and the National Natural Science Foundation of China (Grant No. GG2470000101). X.-F.Z., Z.-W.Z., and G.-C.G. were supported by National Key Research and Development Program (Grant No. 2016YFA0301700), National Natural Science Foundation of China (Grant No. 11574294), and the Strategic Priority Research Program (B) of the Chinese Academy of Sciences (Grant No. XDB01030200).

[1] Z. Fu, L. Huang, Z. Meng, P. Wang, L. Zhang, S. Zhang, H. Zhai, P. Zhang, and J. Zhang, Nat. Phys. **10**, 110 (2014).
[2] L. Zhang, J.-Y. Zhang, S.-C. Ji, Z.-D. Du, H. Zhai, Y. Deng, S. Chen, P. Zhang, and J.-W. Pan, Phys. Rev. A **87**, 011601 (2013).
[3] J.-Y. Zhang, S.-C. Ji, Z. Chen, L. Zhang, Z.-D. Du, B. Yan, G.-S. Pan, B. Zhao, Y.-J. Deng, H. Zhai *et al.*, Phys. Rev. Lett. **109**, 115301 (2012).
[4] L. LeBlanc, M. Beeler, K. Jimenez-Garcia, A. Perry, S. Sugawa, R. Williams, and I. Spielman, New J. Phys. **15**, 073011 (2013).
[5] I. Bloch, J. Dalibard, and W. Zwerger, Rev. Mod. Phys. **80**, 885 (2008).
[6] M. Lewenstein, A. Sanpera, V. Ahufinger, B. Damski, A. Sen, and U. Sen, Adv. Phys. **56**, 243 (2007).
[7] C. Qu, C. Hamner, M. Gong, C. Zhang, and P. Engels, Phys. Rev. A **88**, 021604 (2013).
[8] Y.-J. Lin, R. L. Compton, A. R. Perry, W. D. Phillips, J. V. Porto, and I. B. Spielman, Phys. Rev. Lett. **102**, 130401 (2009).
[9] Y.-J. Lin, R. L. Compton, K. Jimenez-Garcia, J. V. Porto, and I. B. Spielman, Nature (London) **462**, 628 (2009).
[10] M. Beeler, R. Williams, K. Jimenez-Garcia, L. LeBlanc, A. Perry, and I. Spielman, Nature (London) **498**, 201 (2013).
[11] D. Jaksch, C. Bruder, J. I. Cirac, C. W. Gardiner, and P. Zoller, Phys. Rev. Lett. **81**, 3108 (1998).
[12] M. Greiner, O. Mandel, T. Esslinger, T. W. Hänsch, and I. Bloch, Nature (London) **415**, 39 (2002).
[13] M. Greiner, C. A. Regal, and D. S. Jin, Nature (London) **426**, 537 (2003).
[14] T. Bourdel, L. Khaykovich, J. Cubizolles, J. Zhang, F. Chevy, M. Teichmann, L. Tarruell, S. J. J. M. F. Kokkelmans, and C. Salomon, Phys. Rev. Lett. **93**, 050401 (2004).
[15] M. Bartenstein, A. Altmeyer, S. Riedl, S. Jochim, C. Chin, J. H. Denschlag, and R. Grimm, Phys. Rev. Lett. **92**, 120401 (2004).
[16] M. W. Zwierlein, C. A. Stan, C. H. Schunck, S. M. F. Raupach, A. J. Kerman, and W. Ketterle, Phys. Rev. Lett. **92**, 120403 (2004).
[17] C. A. Regal, M. Greiner, and D. S. Jin, Phys. Rev. Lett. **92**, 040403 (2004).
[18] M. W. Zwierlein, C. A. Stan, C. H. Schunck, S. M. F. Raupach, S. Gupta, Z. Hadzibabic, and W. Ketterle, Phys. Rev. Lett. **91**, 250401 (2003).
[19] J. Kinast, S. L. Hemmer, M. E. Gehm, A. Turlapov, and J. E. Thomas, Phys. Rev. Lett. **92**, 150402 (2004).
[20] A. S. Sørensen, E. Demler, and M. D. Lukin, Phys. Rev. Lett. **94**, 086803 (2005).
[21] N. Goldman, A. Kubasiak, A. Bermudez, P. Gaspard, M. Lewenstein, and M. A. Martin-Delgado, Phys. Rev. Lett. **103**, 035301 (2009).
[22] M. A. Baranov, K. Osterloh, and M. Lewenstein, Phys. Rev. Lett. **94**, 070404 (2005).
[23] T. D. Stanescu, B. Anderson, and V. Galitski, Phys. Rev. A **78**, 023616 (2008).
[24] C. Wang, C. Gao, C.-M. Jian, and H. Zhai, Phys. Rev. Lett. **105**, 160403 (2010).
[25] W. Cong-Jun, I. Mondragon-Shem, and Z. Xiang-Fa, Chin. Phys. Lett. **28**, 097102 (2011).
[26] H. Hu, B. Ramachandhran, H. Pu, and X.-J. Liu, Phys. Rev. Lett. **108**, 010402 (2012).
[27] T.-L. Ho and S. Zhang, Phys. Rev. Lett. **107**, 150403 (2011).
[28] Q. Zhou and X. Cui, Phys. Rev. Lett. **110**, 140407 (2013).
[29] Q. Sun, L. Wen, W.-M. Liu, G. Juzeliūnas, and A.-C. Ji, Phys. Rev. A **91**, 033619 (2015).
[30] S.-W. Su, S.-C. Gou, Q. Sun, L. Wen, W.-M. Liu, A.-C. Ji, J. Ruseckas, and G. Juzeliūnas, Phys. Rev. A **93**, 053630 (2016).
[31] M. Gong, S. Tewari, and C. Zhang, Phys. Rev. Lett. **107**, 195303 (2011).
[32] H. Hu, L. Jiang, X.-J. Liu, and H. Pu, Phys. Rev. Lett. **107**, 195304 (2011).
[33] X.-J. Liu and H. Hu, Phys. Rev. A **88**, 023622 (2013).
[34] F. Wu, G.-C. Guo, W. Zhang, and W. Yi, Phys. Rev. Lett. **110**, 110401 (2013).
[35] G. Chen, M. Gong, and C. Zhang, Phys. Rev. A **85**, 013601 (2012).
[36] D. Jaksch and P. Zoller, New J. Phys. **5**, 56 (2003).
[37] A. Celi, P. Massignan, J. Ruseckas, N. Goldman, I. B. Spielman, G. Juzeliūnas, and M. Lewenstein, Phys. Rev. Lett. **112**, 043001 (2014).
[38] F. Gerbier and J. Dalibard, New J. Phys. **12**, 033007 (2010).
[39] N. Goldman, G. Juzeliūnas, P. Öhberg, and I. B. Spielman, Rep. Prog. Phys. **77**, 126401 (2014).
[40] S. Mittal, J. Fan, S. Faez, A. Migdall, J. M. Taylor, and M. Hafezi, Phys. Rev. Lett. **113**, 087403 (2014).
[41] B. M. Anderson, G. Juzeliūnas, V. M. Galitski, and I. B. Spielman, Phys. Rev. Lett. **108**, 235301 (2012).
[42] P. Hauke, O. Tieleman, A. Celi, C. Ölschläger, J. Simonet, J. Struck, M. Weinberg, P. Windpassinger, K. Sengstock, M. Lewenstein *et al.*, Phys. Rev. Lett. **109**, 145301 (2012).
[43] J. P. Vyasanakere, S. Zhang, and V. B. Shenoy, Phys. Rev. B **84**, 014512 (2011).
[44] J. Dalibard, F. Gerbier, G. Juzeliūnas, and P. Öhberg, Rev. Mod. Phys. **83**, 1523 (2011).
[45] Y.-J. Lin, K. Jiménez-García, and I. Spielman, Nature (London) **471**, 83 (2011).
[46] L. W. Cheuk, A. T. Sommer, Z. Hadzibabic, T. Yefsah, W. S. Bakr, and M. W. Zwierlein, Phys. Rev. Lett. **109**, 095302 (2012).
[47] P. Wang, Z.-Q. Yu, Z. Fu, J. Miao, L. Huang, S. Chai, H. Zhai, and J. Zhang, Phys. Rev. Lett. **109**, 095301 (2012).

[48] S. Kolkowitz, S. L. Bromley, T. Bothwell, M. L. Wall, G. E. Marti, A. P. Koller, X. Zhang, A. M. Rey, and J. Ye, Nature (London) **542**, 66 (2017).
[49] X. Luo, L. Wu, J. Chen, Q. Guan, K. Gao, Z.-F. Xu, L. You, and R. Wang, Sci. Rep. **6**, 18983 (2016).
[50] J. Li, W. Huang, B. Shteynas, S. Burchesky, F. Ç. Top, E. Su, J. Lee, A. O. Jamison, and W. Ketterle, Phys. Rev. Lett. **117**, 185301 (2016).
[51] S.-C. Ji, J.-Y. Zhang, L. Zhang, Z.-D. Du, W. Zheng, Y.-J. Deng, H. Zhai, S. Chen, and J.-W. Pan, Nat. Phys. **10**, 314 (2014).
[52] A. J. Olson, S.-J. Wang, R. J. Niffenegger, C.-H. Li, C. H. Greene, and Y. P. Chen, Phys. Rev. A **90**, 013616 (2014).
[53] C. Hamner, C. Qu, Y. Zhang, J. Chang, M. Gong, C. Zhang, and P. Engels, Nat. Commun. **5**, 4023 (2014).
[54] L. Huang, Z. Meng, P. Wang, P. Peng, S.-L. Zhang, L. Chen, D. Li, Q. Zhou, and J. Zhang, Nat. Phys. **12**, 540 (2016).
[55] Z. Wu, L. Zhang, W. Sun, X.-T. Xu, B.-Z. Wang, S.-C. Ji, Y. Deng, S. Chen, X.-J. Liu, and J.-W. Pan, Science **354**, 83 (2016).
[56] H. Lignier, C. Sias, D. Ciampini, Y. Singh, A. Zenesini, O. Morsch, and E. Arimondo, Phys. Rev. Lett. **99**, 220403 (2007).
[57] A. Zenesini, H. Lignier, D. Ciampini, O. Morsch, and E. Arimondo, Phys. Rev. Lett. **102**, 100403 (2009).
[58] F. Meinert, M. J. Mark, K. Lauber, A. J. Daley, and H.-C. Nägerl, Phys. Rev. Lett. **116**, 205301 (2016).
[59] B. Huang, P. H. Chui, J. Liu, C. Zhang, and M. Gong, arXiv:1511.01713.
[60] T. Morimoto and A. Furusaki, Phys. Rev. B **88**, 125129 (2013).
[61] M. Ueda, *Fundamentals and New Frontiers of Bose-Einstein Condensation* (World Scientific, Singapore, 2010).
[62] Q. Zhou, J. V. Porto, and S. Das Sarma, Phys. Rev. A **84**, 031607 (2011).
[63] W. Zheng, B. Liu, J. Miao, C. Chin, and H. Zhai, Phys. Rev. Lett. **113**, 155303 (2014).
[64] A. P. Schnyder, S. Ryu, A. Furusaki, and A. W. W. Ludwig, Phys. Rev. B **78**, 195125 (2008).
[65] S. Ryu, A. P. Schnyder, A. Furusaki, and A. W. Ludwig, New J. Phys. **12**, 065010 (2010).
[66] L. Ortiz and M. A. Martin-Delgado, Ann. Phys. (NY) **375**, 193 (2016).
[67] K. S. Novoselov, E. McCann, S. Morozov, V. I. Fal'ko, M. Katsnelson, U. Zeitler, D. Jiang, F. Schedin, and A. Geim, Nat. Phys. **2**, 177 (2006).
[68] E. McCann and V. I. Fal'ko, Phys. Rev. Lett. **96**, 086805 (2006).